Special Issue of the 8th International Advances in Applied Physics and Materials Science Congress (APMAS 2018)

Effect of Time and Temperature on the Sensitization on Alloy 600 by Electrochemical Potentiokinetic Reactivation

K.H. Jung and S.J. Kim*

Mokpo National Maritime University, Division of Marine Engineering, Mokpo, Korea

This study investigated the effect of temperature and time on the sensitization behavior of alloy 600. A double-loop electrochemical potentiokinetic reactivation test was conducted to evaluate the degree of sensitization (DOS) in 0.1 M H_2SO_4 + 0.001 M potassium thiocyanate solution. The microstructure and surface damages of the aged specimens were characterized by optical microscope, scanning electron microscope, and energy dispersive X-ray spectroscopy. As a result of the experiment, the sensitization behavior was significantly influenced by the expansion of the Cr-depleted zone and Cr-diffusion rate depending on the aging temperature. In particular, the alloy 600 aged for 300 h or longer at 650 °C represented a very low DOS value of 3% or less, and its resistance against intergranular corrosion greatly improved.

DOI: 10.12693/APhysPolA.135.999

PACS/topics: sensitization, alloy 600, electrochemical potentiokinetic reactivation, Cr-rich carbide

1. Introduction

Stainless steel and nickel alloy are very vulnerable to the sensitization phenomenon [1–4]. Sensitization is that, as the alloy is exposed to a temperature range of 550–850 °C for a certain period of time, Cr-rich carbides are precipitated on the grain boundaries of the alloy structure, thus forming a Cr depletion zone. If the Cr content around the grain boundaries is reduced to 12% or less, the formation of protective Cr-oxide films becomes unstable [3, 4], which makes the metal vulnerable to the corrosion attack. In general, the higher the Ni content in an alloy is, the lower the carbon solubility becomes [1, 2, 5]. This causes the supersaturated carbon to react with the alloy elements in the sensitization temperature range and accelerates the nucleation and growth of the carbides. Thus, the alloy will be easily sensitization [5]. Among nickel alloys, alloy 600 is widely used as a tube material for the pressurized water reactor (PWR) in nuclear power plants. Owing to its excellent corrosion resistance and mechanical properties compared to stainless steel, it is widely used in various industries such as chemical facilities, power-generating facilities, and marine facilities. However, intergranular corrosion and stress corrosion cracking frequently occur due to sensitization under high temperature environments such as the tube material for steam generators for PWRs. This durability problem of this material has a critical effect on the lifespan, durability, and stability of facilities and equipment. Thus, studies of sensitization of alloy 600 have been researched for many years [5–11]. One of the most frequently used sensitization test methods for stainless steel is electrochemical potentiokinetic reactivation (EPR), which is a quantitative nondestructive method. First proposed by Chihal [12], this method has been used for the research on sensitization of alloys by many researchers. Among the EPR methods, the Double-Loop Electrochemical Potentiokinetic Reactivation (DL-EPR) is used very often because it is less sensitive to the surface treatment and inclusions of alloys [13]. Furthermore, many studies on the sensitization and intergranular corrosion of alloy 600 have been conducted by the DL-EPR method. However, the studies on the sensitization and intergranular corrosion of alloy 600 are mainly concentrated on short-term phenomena such as welding [14], heat treatment [6], and processing [9, 10], while there is no study on sensitization study using specimens aged for 100 h or more. The design lifespan of metal materials generally ranges from several years to several decades. Besides, the sensitization rate is strongly dependent on the temperature of the applied environment. Therefore, evaluation on the sensitization of alloy 600 used over a long period is indispensable. The purpose of this study is to evaluate the effects of long-term degradation and temperature on the sensitization behavior of alloy 600. In this study, the sensitization behavior of alloy 600 was evaluated after it had been aged at 650 °C for up to 1,000 h.

2. Materials and equipments

The chemical composition [wt. %] of alloy 600 used in this experiment is 0.01 C, 0.05 Si, 0.14 Mn, 15.3 Cr, 0.5 Cu, 0.015 S, and Ni for the rest. The isothermal aging was performed until 1,000 h at 550 °C and 650 °C, using an electric furnace for heat treatment. The specimens for observation of the microstructure were grinded with SiC paper of up to grit #2000 and were polished by using 0.3 μm alumina powder. The microstructure and chemical composition of carbides were characterized by using a scanning electron microscope (SEM) and energy dispersive X-ray spectroscopy (EDS) after the specimens were etched using aqua regia (HNO_3 + HCl) solution until the grain boundaries were revealed.

*corresponding author; e-mail: ksj@mmu.ac.kr

The DL-EPR experiment was performed by using PIC4 of Gamry Co. The electrochemical cell was composed with a platinum electrode as a counter and Ag/AgCl (saturated KCl) electrode as a reference. The solution used was 0.1 M $H_2SO_4 + 0.001$ M potassium thiocyanate (KSCN) of 25 °C. The specimens (1 cm × 1 cm) for the electrochemical test were polished up to #2000 using emery paper and then washed with ethanol and distilled water. The open-circuit potential (OCP) was measured after immersing the specimen in the solution for 2 min. For polarization, the forward scan was performed at a scan rate of 1.67 mV/s from the OCP to 600 mV (vs. SSE) and then, reverse scan was performed back to OCP at the same scan rate. The DOS was calculated by the ratio of reverse scan peak (I_r) to anodic scan peak (I_a), i.e.

$$\text{DOS} = I_r/I_a \times 100\%.$$

The DL-EPR test was performed at least three times at each condition to ensure reproducibility.

3. Results and discussion

To observe the effect of KSCN on intergranular corrosion, the DL-EPR test was conducted on alloy 600 specimens in 0.1 M H_2SO_4 + 0.001 M KSCN solution [8]. The results are shown in Fig. 1. The behavior of the polarization curve (Fig. 1a) varied significantly with the addition of KSCN. In the case of 0.1 M H_2SO_4 + 0.001 M KSCN solution (Fig. 1b), the open-circuit potential moved to the active direction, while the peak values of the anodic loop and reactivation loop increased sharply. The reason is that KSCN acts as a strong activator in the solution and also as a depassiving agent which destroys the vulnerable passivity on the Cr-depleted zone during the reactivation process [10]. No surface damage was observed in the specimen corroded in the 0.1M H_2SO_4 solution (Fig. 1c). On the other hand, heavy intergranular and pitting damage was observed in the specimen corroded in the 0.1 M H_2SO_4 + 0.001 M KSCN solution as KSCN chemically attacked surrounding carbides on the grain boundaries and matrix. This is consistent with the result of a study by Lim et al. [10]. In general, if the DOS is 5% or higher, the alloy is regarded as sensitized [12]. In this study, the base metal represented a very high DOS value of 10.48%. This is considered as sensitization of the material itself which occurred in the manufacturing and heat treatment process, not from an inappropriate selection of the DL-EPR test condition [5].

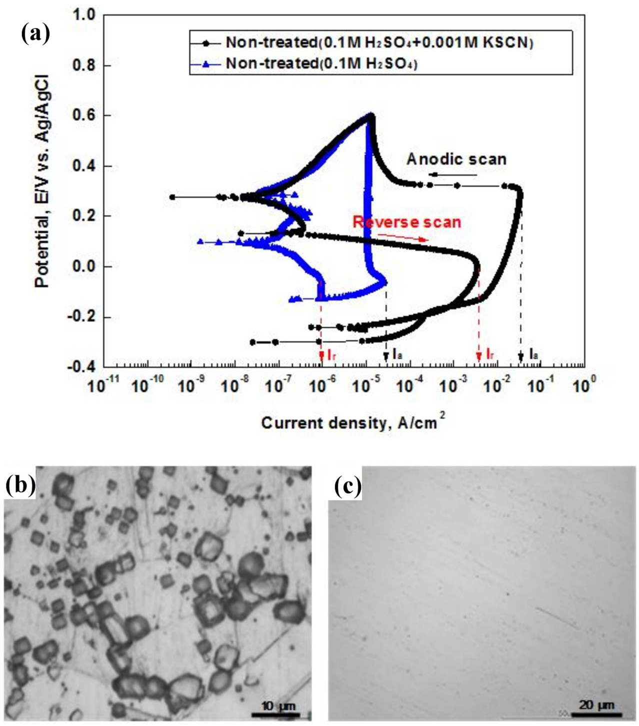

Fig. 1. Result of the DL-EPR test for non-aged alloy 600 with or without KSCN addition, (a) polarization curve, (b) 0.1 M H_2SO_4, (c) 0.1 M H_2SO_4 + 0.001M KSCN.

To evaluate the sensitization on the intergranular corrosion of alloy 600 which was isothermally aged at 550 °C and 650 °C, the DL-EPR test was performed in 0.1 M H_2SO_4 + 0.001 M KSCN solution. Figure 2 shows a DL-EPR curve with aging time, and the detailed values are listed in Tables I, II. The difference between electric potentials represented by I_a and I_r values is considered to have been affected by drop in the Ohmic resistance [15]. The I_a values were similar regardless of the aging conditions, whereas I_r values drastically changed depending on the temperature and time of aging. At 550 °C, the I_r value showed a sharply increasing tendency with the progress of aging (Table I). An increase of the I_r value implies chemical damage in the Cr-depleted zone and matrix structure, indicating the increase of the DOS value of the material. Meanwhile, the I_r values of the specimens aged at 650 °C showed a sharply decreasing tendency after 200 h. Consequently, alloy 600 aged at 650 °C represented a lower I_r value than that of the base metal with a critical point of approximately 200 h.

TABLE I

Detailed value of the I_r, I_a, and DOS for the alloy 600 aged at 550 °C.

	I_r, [A/cm^2]	I_a, [A/cm^2]	DOS, [%]
untreated	3.45×10^{-3}	3.29×10^{-2}	10.48
100 h	1.47×10^{-2}	3.79×10^{-2}	38.88
200 h	1.44×10^{-2}	3.85×10^{-2}	37.54
300 h	1.86×10^{-2}	4.23×10^{-2}	44.04
500 h	1.78×10^{-2}	4.01×10^{-2}	44.38
700 h	1.78×10^{-2}	3.72×10^{-2}	47.92
1000 h	1.88×10^{-2}	4.19×10^{-2}	44.79

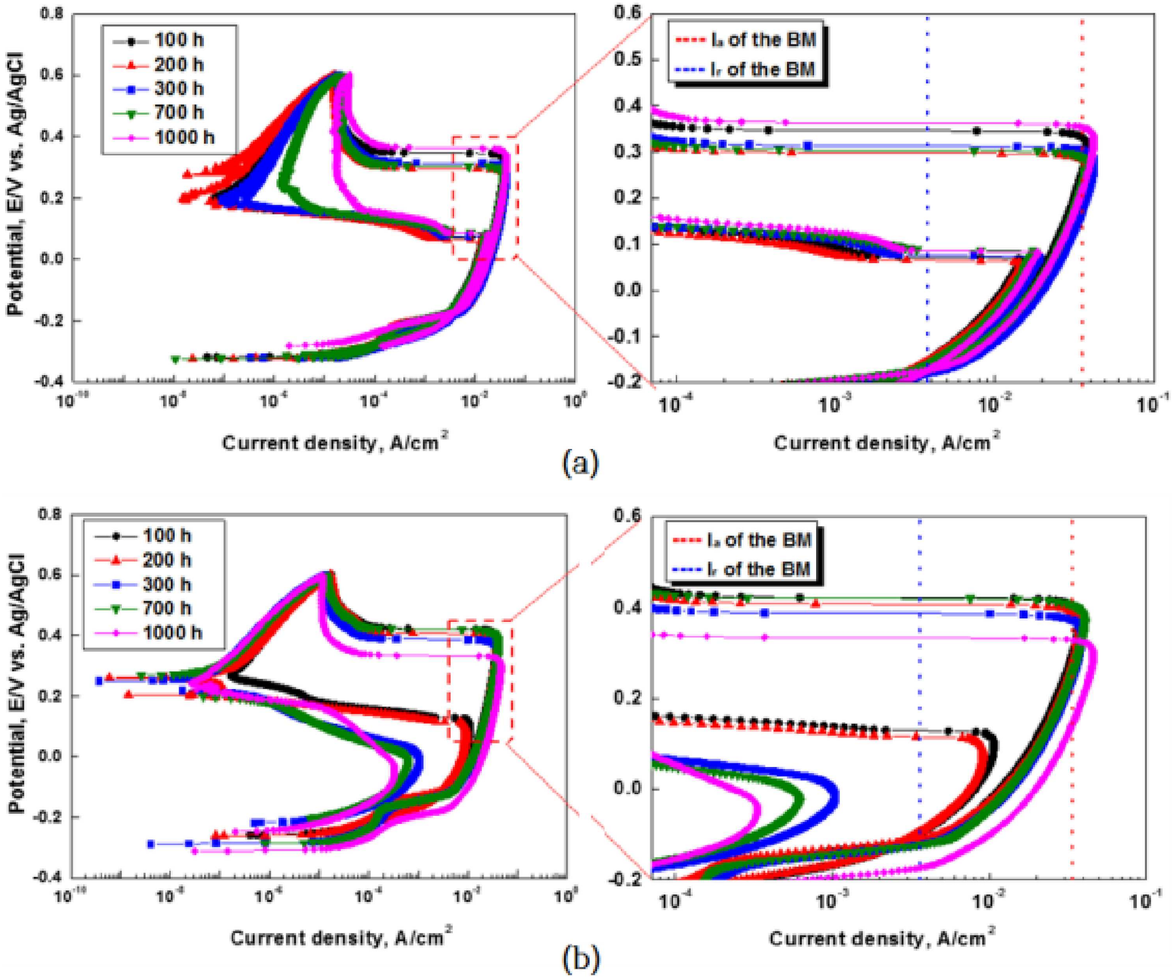

Fig. 2. DL-EPR curves and comparison of the current peak (I_r and I_a) of the alloy 600 with aging time, (a) aged at 550 °C, (b) aged at 650 °C.

TABLE II

Detailed value of the I_r, I_a, and DOS for the alloy 600 aged at 650 °C.

	I_r, A/cm^2	I_a, A/cm^2	DOS, %
100 h	1.07×10^{-2}	3.74×10^{-2}	28.61
200 h	9.06×10^{-3}	3.80×10^{-2}	23.81
300 h	1.04×10^{-3}	3.88×10^{-2}	2.68
500 h	1.14×10^{-3}	4.47×10^{-2}	2.55
700 h	6.15×10^{-4}	4.04×10^{-2}	1.52
1000 h	3.33×10^{-4}	4.59×10^{-2}	0.72

Figure 3 presents images of the microstructure of alloy 600 aged at 650 °C. In the case of the specimen aged for 300 h (Fig. 3a), carbides in nm scale were precipitated in dual shapes (no continuous carbide) along the grain boundaries. The EDS composition analysis for carbide (Fig. 3b) showed that Cr and C contents are 21.39 % and 8.1 % respectively, which are much higher than those of the matrix (Fig. 3d). It means that the carbide precipitated on the isothermally aged alloy 600 are Cr-rich carbides (M_7C_3, $M_{23}C_6$) [9]. In general, the carbides precipitated on austenitic alloys grow in the process: step (absence of chromium carbide) → dual (no discontinuous carbide) → ditch (surrounded by ditch). However, in this study, the nucleation and growth of carbides tended to stagnate after 300 h of aging (Fig. 3b). According to previous studies [7, 16], M_7C_3 and $M_{23}C_6$ carbides grow in accordance with the Ostwald ripening mechanism during the isothermal aging process. This is because the supersaturated carbon content required for carbide formation is limited to some degree [1, 2, 16]. As a result, the nucleation and growth of Cr-rich carbides are inevitably limited during the isothermal aging. The carbon content of the alloy used in this study is 0.0145 wt%, and it seems that most of the nucleation and coarsening took place within 300 h.

Figure 4 represents images of the surface with aging time after DL-EPR test for specimens aged at 550 °C. The DOS value is generally proportional to the length and width of the Cr-depleted zone [6]. In this study as well, the depth and width of the intergranular damage increased in proportion to the DOS value. At 100 h (DOS 38.88%), which is an early stage of aging distinct

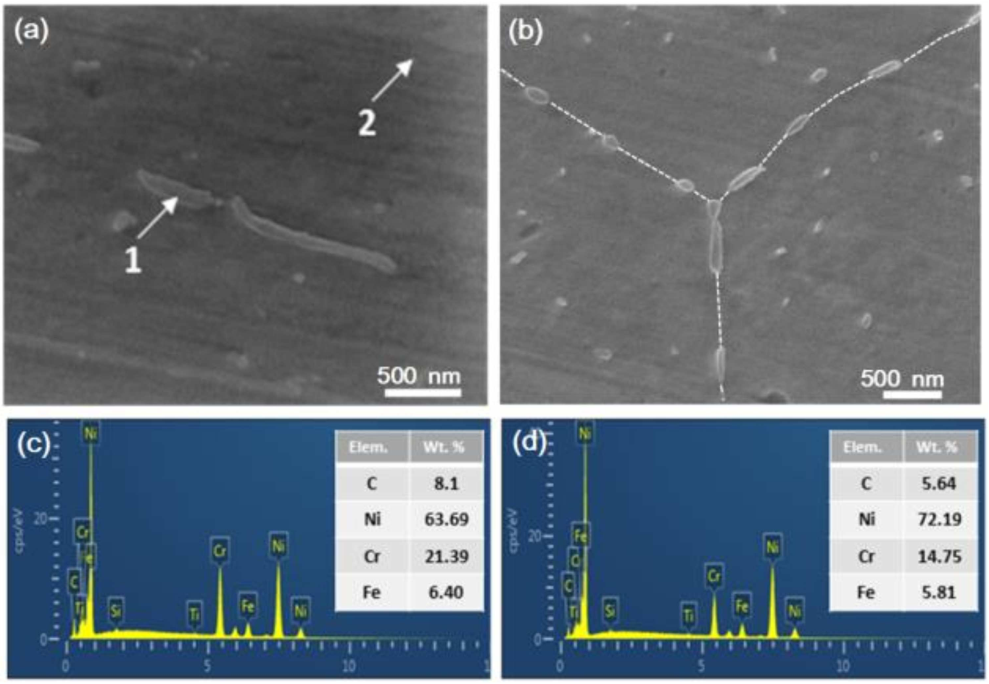

Fig. 3. Results of SEM and EDS analysis on the precipitates in alloy 600 aged at 650 °C (a) 300 h, (b) 1000 h, (c) EDS result of the spot 1, (d) EDS result of the spot 2.

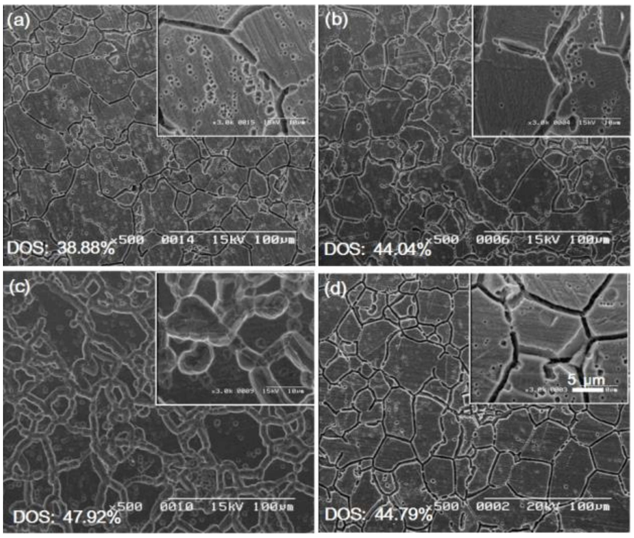

Fig. 4. Surface morphologies of the alloy 600 aged 550 °C after DL-EPR test with aging time, (a) 100 h, (b) 300 h, (c) 700 h, (d) 1000 h.

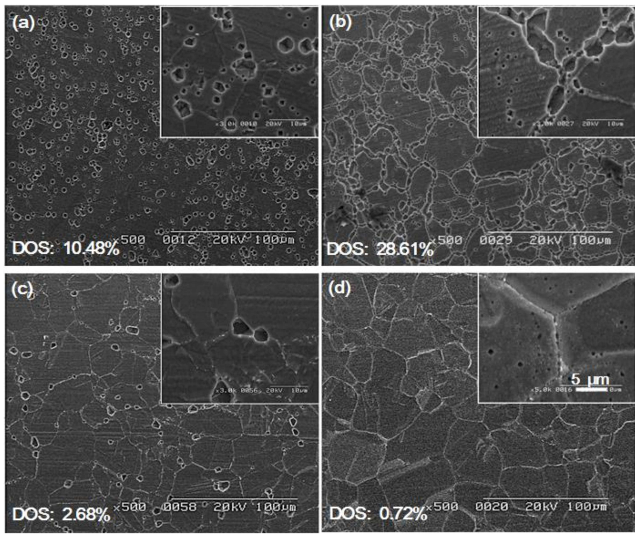

Fig. 5. Surface morphologies of the alloy 600 aged 650 °C after DL-EPR test with aging time, (a) non-aged, (b) 100 h, (c) 300 h, (d) 1000h.

ditch-shaped intergranular damages and many pitting damages were observed in the grains (Fig. 4a), and the width of the ditch-shaped damages showed an increasing trend with the progress of aging time (Fig. 4b, c). In the case of the specimen that had been aged for 700 h which showed the largest DOS value, the largest surface damage was observed. However, the surface damage of the specimen aged for 1000 h (Fig. 4d) was somewhat reduced. It is considered that the de-sensitization appears by the self-healing effect due to the Cr diffusion.

Figure 5 shows images of the surface with the aging time after the DL-EPR test for specimens aged at 650 °C. The base metal in Fig. 5a exhibited the structure of end grain pitting I in which multiple deep end grain pits and shallow etch pits appear. They are caused by the preferential dissolution of the local Cr-depletion zone formed around the Cr-rich carbides precipitated at the grain boundaries and matrix in the reactivation process. In the specimen aged for 100 h in Fig. 5b (DOS 28.61%), a ditch-shaped damage was observed, which is a typical damage of intergranular corrosion. After the largest intergranular and pitting damages were observed at 100 h of aging, the damages showed a rapidly decreasing tendency with the increasing aging time (Fig. 5c, d). In the specimen aged for 1000 h (DOS 0.72%), only very small pitting damages were observed in the grains due to desensitization, and it showed the best surface in this study. In general, the surface damages were highly consistent with the DOS values in Table II.

Figure 6 depicts the analysis results of the surface with an EDS element map after the DL-EPR test for specimens aged at 550 °C for 700 h and at 650 °C for 1000 h. First, in the specimens aged at 550 °C for 700 h (Fig. 6a), oxygen (O) and Cr were detected uniformly on the surface (Fig. 6b, c). This implies the formation of thin, uniform Cr-rich oxide films on the surface during the anodic scan process in the DL-EPR test. However, no O were detected along the ditch-shaped damage, which suggests destroying the passivation by KSCN. The intergranular Cr-rich carbides seem to have been mostly detached during the dissolution process. Furthermore, it can be seen that there is a Cr depletion zone along the grain boundaries through the brightness gradient in the Cr element map. Meanwhile, in the case of the specimen aged at 650 °C for 1000 h (Fig. 6d), the DOS value is 0.72%, and a very good surface was observed. Furthermore, the existence of intact Cr-rich carbides at the grain boundaries could be verified through SEM images and Cr element map (Fig. 6e). Even though Cr depletion certainly happened in the periphery by the formation of Cr-rich carbides, intact Cr-rich oxide films were maintained. This is because the Cr depletion zone was reduced by the self-healing phenomenon due to the above-mentioned Cr diffusion effect.

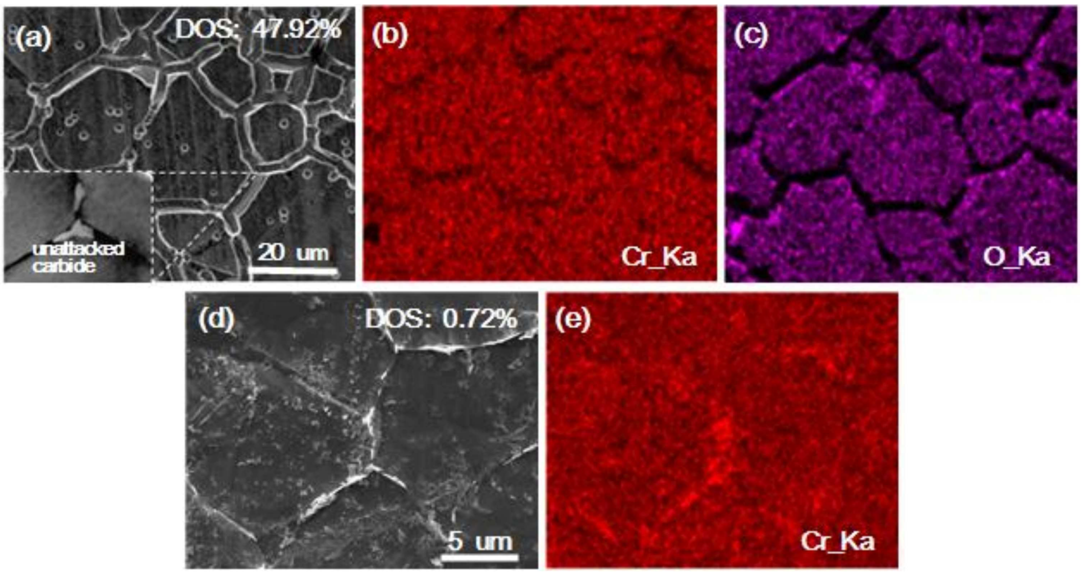

Fig. 6. SEM micrographs and EDS element mapping of isothermally aged alloy 600 after DL-EPR test, (a) 550 °C–700 h, (b) Cr elemthe ent map of (a), (c) O element map of (a), (d) 650 °C–1000 h, (e) Cr element map of (d).

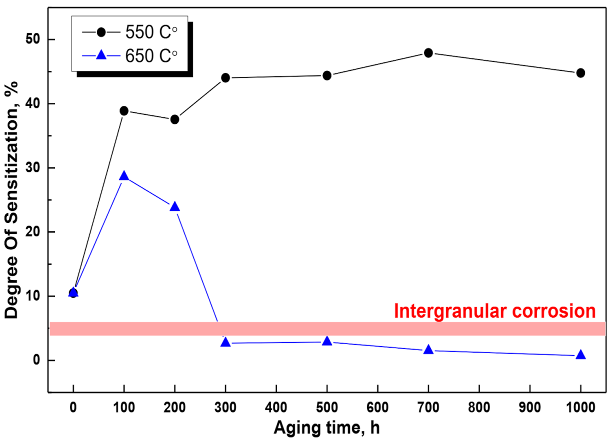

Fig. 7. Comparison schematics of the DOS values for alloy 600 isothermally aged at 550 °C and 650 °C.

Figure 7 compares DOS values by aging temperature and time. The expansion of the Cr depleted zone in the isothermal aging process is caused by the complex effects of the precipitation of Cr-rich carbides and the Cr diffusion (self-healing) by the difference in alloy element concentration between the matrix and the depleted zone [13]. The production and growth of Cr-rich carbides accelerate the expansion of the Cr depletion zone by consuming Cr in the periphery. On the other hand, the diffusion of Cr by the difference in concentration between the matrix structure and the depleted zone prevents the growth of the Cr-depleted zone. These two factors have mutually competing relations in the isothermal process and determine the expansion speed of the Cr-depleted zone [9]. Due to these two phenomena, the behavior of the DOS values by temperature and time showed different tendencies. First, at 550 °C, the DOS value presented a sharply increasing tendency at 100 h. This is because the Cr-depleted zone in the surrounding of grain boundaries is quickly expanding due to the rapid nucleation and growth of Cr-rich carbides, and it is impossible for the Cr in the matrix to sufficiently spread to the depleted zone [6, 9, 11]. However, the DOS value tended to drastically decrease from 200 h of aging. In conclusion, in the case of specimens aged at 650 °C, the largest DOS value was measured at 28.61% at 100 h of aging, but the DOS value decreased sharply with the progress of aging. The reason is that as most of the supersaturated carbons are precipitated as Cr-rich carbides, the Cr diffusion rate is faster than the Cr consumption rate [6, 11]. Thus, alloy 600 showed a rapidly decreasing tendency of DOS due to the self-healing phenomenon resulting from the diffusion of Cr after 100 h at 650 °C [7]. Moreover, the alloy presented a very small DOS value of less than 3% from 300 h, indicating improved resistance to sensitization and intergranular corrosion.

4. Conclusion

The carbides precipitated at the grain boundaries during isothermal aging were confirmed to be Cr-rich carbides in the type of M_7C_3 and $M_{23}C_6$. However, alloy 600 which was used in this study showed a tendency of limited nucleation and growth of Cr-rich carbides by aging after a certain time due to the low carbon content. The sensitized alloy 600 steel showed ditch-shaped intergranular damages and many pitting damages in the matrix. The EDS map analysis revealed the formation of a Cr-depleted zone along the ditch-shaped damage. The surface damages and DOS values were very consistent. The sensitization behavior of alloy 600 in the DL-EPR test presented different tendencies depending on the aging temperature and time. At 550 °C, the DOS value showed an increasing tendency as the aging time increased. On the other hand, at 650 °C, the DOS value decreased sharply as the Cr diffusion prevailed rather than the expansion of Cr-depleted zone after 100 h, and a very low DOS value of less than 3% was measured after 300 h.

Acknowledgments

This research was a part of the project titled "Build a clean thermal power generation demonstration test bed", funded by the Ministry of Trade, Industry and Energy, Korea (No. 20161110100090).

References

[1] A.J. Sedriks, *Corrosion of stainless steel*, 2nd ed., Wiley-Interscience, New York 1996.

[2] D.A. Jones, *Principles and prevention of corrosion*, Pearson Education, 1996.

[3] E.R. Hwang, B.H. Seo, S.G. Kang, *J. Kor. Inst. Surf. Eng.* **31**, 223 (1998).

[4] H.C. Choe, J. Kor. *J. Kor. Inst. Surf. Eng* **37**, 350 (2004).

[5] S. Kumar, B.S. Prasad, V. Kain, J. Reddy, *Corros. Sci.* **70**, 55 (2013).

[6] G.S. Was, H.H. Tischner, R.M. Latanision, *Metall. Mater. Trans. A* **12**, 1397 (1981).

[7] E.L. Hall, C.L. Briant, *Metall. Mater. Trans. A* **16**, 1225 (1985).

[8] M.F. Maday, A. Mignone, M. Vittori, *Corros. Sci.* **28**, 887 (1988).

[9] J.J. Kai, C.H. Tsai, G.P. Yu, *Nucl. Eng. Des.* **144**, 449 (1993).

[10] Y.S. Lim, H.P. Kim, J.H. Han, J.S. Kim, H.S. Kwon, *Corros. Sci.* **43**, 1321 (2011).

[11] H. Li, J.R. Ma, X.R. Liu, S. Xia, W.Q. Liu, B.X. Zhou, *Mater. Sci. Forum* **879**, 1111 (2017).

[12] ISO 12732, Corrosion of Metals and Alloys – Electrochemical Potentiokinetic Reactivation Measurement Using the Double Loop Method (Based on the Cihal Method), 1st ed., Geneva, Switzerland 2006.

[13] S. Zhang, Z. Jiang, H. Li, H. Feng, B. Zhang, *J. Alloys Compd.* **695**, 3083 (2017).

[14] A. Srikanth, M. Manikandan, *J. Manuf. Process.* **30**, 452 (2017).

[15] A.P. Majidi, M.A. Streicher, *Corros.* **40**, 584 (1984).

[16] F. Abe, *Mater. Sci. Eng. A* **15**, 565 (2004).